JOURNAL OF Materials CHEMISTRY

Structure and physical properties of a hydrogen-bonded self-assembled material composed of a carbamoylmethyl substituted TTF derivative

Go Ono,[a] Akira Izuoka,[a] Tadashi Sugawara*[a] and Yoko Sugawara[b]

[a]*Department of Basic Science, Graduate School of Arts and Sciences, the University of Tokyo, Komaba, Meguro, Tokyo 153, Japan*

[b]*School of Science, Kitasato University, Sagamihara, Kanagawa 288, Japan*

Crystal structures of the carbamoylmethyl substituted TTF derivative AMET are characterized by polymeric hydrogen bonding between amide groups. As a result, the TTF moieties stack in parallel even in the neutral crystal. The ν_{NH} absorbtions of neutral AMET at 3426 and 3184 cm^{-1} show shifts to lower wavenumber, Δk, of 37 and 58 cm^{-1}, respectively, at 4.1 GPa. Therefore the shrinkage of the N—H···O distance is estimated to be *ca.* 0.04 Å at this pressure. The pressure dependence of the IR spectra of iodine-doped samples at doping ratios of less than 45% was exactly the same as that for a neutral sample, suggesting that the hydrogen bonding pattern is not affected significantly upon doping.

Although crystalline AMET is an insulator in the neutral state ($\sigma_{rt} = ca.\ 10^{-8}$ S cm^{-1}), the conductivity is enhanced by a factor of 10^7 upon iodine doping of 45 mol% ($\sigma_{rt} = 1.2 \times 10^{-1}$ S cm^{-1}). Furthermore, the conductivity increases as a function of the external pressure, and the σ_{rt} of a 5% iodine-doped sample increased three-fold at 1.0 GPa. The enhanced conductivity of iodine-doped samples may be ascribed to the increase in the overlap between the donor moieties based on the shrinkage of the hydrogen bond of the carbamoylmethyl group.

Construction of molecular self-assemblies has become a current topic of interest in materials chemistry.[1] Although various sophisticated molecular architectures are now known, the number of molecular assemblies which exhibit prominent functionalities is still limited. In this respect, it may be interesting to design a novel organic donor as a building block for the self-assembly, the functionalities of which can be controlled by means of external stimuli.[2]

It is well-known that organic donors, *e.g.* perylene, TTF, BEDT-TTF and TMTSF, prefer to align in a herringbone structure in the neutral state in order to avoid electronic repulsion between π-electron rich donor molecules.[3] On the other hand, when the donors are partially oxidized, they tend to stack one above the other, with intermolecular contacts between heavy atoms, *e.g.* sulfur or selenium. The heteroatom contacts, then, construct conduction paths by themselves, as long as the HOMO of the donor has reasonably large coefficients on these heteroatoms.[4] If a stacking structure can be obtained even for the neutral donors by means of specific intermolecular forces, the molecular assembly is expected to exhibit controllable transportational phenomena by hole-doping, application of an external pressure, *etc.*

In this respect, we were intrigued by the hydrogen-bonded crystal structures of primary amides.[5,6] The crystal structure of benzamide is characterized by a one-dimensional chain composed of a doubly hydrogen-bonded dimers; the dimer is formed *via* one of the amide hydrogens, while the other amide hydrogen forms a polymeric hydrogen-bonded chain[6] (Fig. 1). Moreover, the one-dimensional arrangement of the phenyl ring of benzamide in the crystal is entirely different from a typical herring-bone type packing, as observed in crystals of aromatic hydrocarbons. Hydrogen-bonded molecular assemblies constructed using amide groups, therefore, are likely to be effective for regulating the structure of molecular self-assemblies composed of organic donors.

Bryce and co-workers reported a TTF derivative substituted with a thioamide group.[7] Although a polymeric hydrogen-bonded chain is constructed by the thioamide groups, the packing of the donor moieties is of a herringbone type. Since the thioamide group is directly attached to the donor moiety, the direction of the hydrogen bond is restricted to the horizontal direction with reference to the donor plane. Thus the packing pattern is not significantly influenced by the hydrogen bond of the thioamide group.

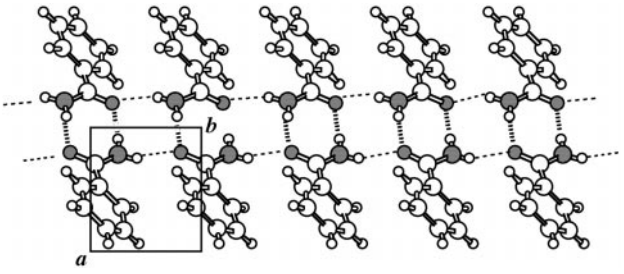

Fig. 1 Crystal structure of benzamide viewed along the *c* axis

Recently, we have prepared BEDT-TTF derivative AMET **1** carrying a carbamoylmethyl group (CH_2CONH_2). The difference in the conformations of the hydrogen-bonding groups between thioamide TTF and AMET may be explained by the presence of a methylene unit between the amide group and the donor moiety; the hydrogen bond in AMET is expected to be formed perpendicular to the donor plane due to the flexibility of the carbamoylmethyl group.

In the present paper, the hydrogen-bonding scheme of neutral crystals of AMET is investigated by X-ray crystallography and IR spectroscopy. The conducting behavior of iodine-doped AMET is measured as a function of the doping ratio. The change in the hydrogen-bonding scheme of the iodine-doped sample is also examined by IR spectroscopy. Finally the effect of external pressure on the conductivity and the hydrogen bonding scheme of AMET is investigated with reference to the possible pressure control of the transportation properties of hydrogen-bonded organic conducting materials.

Experimental

Materials

Syntheses of zinc chelate **8**,[8,9] 4,5-ethylenedithio-1,3-dithiol-2-one **2**[8] and 4-acetylthio-5-methylthio-1,3-dithiole-2-thione **5**[10]

were performed according to published procedures. Tetrahydrofuran (THF) was distilled over sodium metal in the presence of benzophenone prior to use under a nitrogen atmosphere. Methanol was distilled under a nitrogen atmosphere after an addition of sodium metal. Dichloromethane and 1,1,2-trichloroethane were treated with sulfuric acid, then washed with saturated aqueous $NaHCO_3$, water and brine, successively. The solvents were distilled after being dried over $CaCl_2$ for several hours at room temperature. Acetone, 2-bromoethanol and 1,3-dibromopropane were treated with K_2CO_3 and distilled. Triethyl phosphite was dried over sodium metal and distilled under a nitrogen atmosphere. All other reagents were used as purchased without further purification.

Gel permeation chromatography was performed using an LC-08 instrument (Japan Analytical Industry Co., Ltd.) equipped with JAIGEL-1H and -2H columns. Chloroform was used as eluent.

Cyclic voltammetry

Cyclic voltammograms (CVs) were measured in dichloromethane in the presence of tetrabutylammonium perchlorate (0.1 mol l^{-1}) as electrolyte with a platinum working electrode using a potentiostat/galvanostat HAB 151 (HOKUTO DENKO Ltd.). An Ag/AgCl electrode was used as the reference electrode. The scanning rate was 200 mV s^{-1}.

Spectral measurements

^1H NMR spectra were measured using a JEOL GSX-270 spectrometer; chemical shifts in $CDCl_3$ solution are reported in δ units relative to tetramethylsilane as internal standard. UV–VIS–NIR spectra were measured using a Nihon Bunko V-570 series UV–VIS–NIR spectrometer using KBr pellets. Infrared spectra were recorded using a Perkin-Elmer 1400 series infrared spectrometer using KBr pellets. The pressure dependence of the IR spectra was measured by pressing a KBr pellet using a diamond anvil cell.

Preparation

4-(2-Ethoxycarbonylethylthio)-5-methylthio-1,3-dithiole-2-thione 6. In a 200 ml round-bottomed, short-necked flask fitted with a dropping funnel, 4-acetylthio-5-methylthio-1,3-dithiole-2-thione **5** (3.60 g, 15.1 mmol) was dissolved in 100 ml of methanol, and the flask was cooled with an ice bath. To this solution was added dropwise sodium methoxide (820 mg, 15.1 mmol) in 20 ml of methanol with stirring under nitrogen. The resulting red solution was stirred for 1 h at room temperature. The solution was cooled with an ice bath again, and ethyl 3-bromopropionate (2.73 g, 15.1 mmol) in 20 ml of methanol was added under nitrogen. The mixture was stirred for 12 h at room temperature. The solvent was evaporated and the residue was extracted with dichloromethane to remove sodium bromide. The orange solution was washed with 150 ml of saturated aqueous $NaHCO_3$ and 150 ml of water twice. The mixture was dried over anhydrous $MgSO_4$ and filtered, and then the solvent was evaporated. The product, 4-(2-ethoxycarbonylethylthio)-5-methylthio-1,3-dithiole-2-thione **6**, was obtained as a yellow oil (4.45 g, 14.2 mmol, 93%); δ_H ($CDCl_3$) 1.28 (t, $J=7.3$ Hz, 3H), 2.53 (s, 3H), 2.70 (t, $J=7.3$ Hz, 2H), 3.11 (t, $J=7.3$ Hz, 2H), 4.19 (q, $J=7.3$ Hz, 2H); ν_{max}(KBr)/cm^{-1} 2982, 2928 (CH_2), 1733 (C=O, ester), 1423 (C=C), 1029 (C=S), 744 (C−S−C).

4-(2-Ethoxycarbonylethylthio)-5-methylthio-1,3-dithiole-2-one 3. In a 200 ml round-bottomed, short-necked flask, (4.45 g, 14.2 mmol) and mercury(II) acetate (13.60 g, 42.7 mmol) were dissolved in 20 ml of acetic acid and 60 ml of chloroform. The mixture was stirred for 3 h at room temperature. The mixture was filtered to remove mercury salts, and the filtrate was washed with 100 ml saturated aqueous $NaHCO_3$ and 100 ml of water twice. The solution was dried over anhydrous $MgSO_4$ and filtered, and the solvent was evaporated under reduced pressure. The product was purified by column chromatography with silica gel using chloroform–hexane (1:1) as eluent. Evaporation of the solvent gave **3** as a yellow oil (4.00 g, 13.5 mmol, 95%); δ_H($CDCl_3$) 1.29 (t, $J=7.3$ Hz, 3H), 2.48 (s, 3H), 2.69 (t, $J=7.3$ Hz, 2H), 3.10 (t, $J=7.3$ Hz, 2H), 4.18 (q, $J=7.3$ Hz, 2H); ν_{max}(KBr)/cm^{-1} 2982 and 2924 (CH_2), 1733 (C=O, ester), 1669 (C=O, 1,3-dithiol-2-one), 1425 (C=C), 1186 and 1022 (C−O), 741 (C−S−C).

4,5-Ethylenedithio-4′-(2-ethoxycarbonylethylthio)-5′-methylthiotetrathiafulvalene 4. In a 100 ml round-bottomed, short-necked flask fitted with an air condenser, **2** (2.81 g, 13.5 mmol) and **3** (4.00 g, 13.5 mmol) were dissolved in 20 ml of triethyl phosphite. The mixture was heated in an oil bath at 110 °C with stirring for 3 h under nitrogen. The solvent and triethyl phosphate were then evaporated under reduced pressure at 100 °C. The resulting red residue was extracted with chloroform and filtered off with suction to remove BEDT-TTF. The product **4** was separated from homo-coupled TTF derivatives by silica gel column chromatography using dichloromethane–hexane (3:7) as eluent. Evaporation of the solvent gave **4** as red oil (1.76 g, 3.72 mmol, 23%); δ_H($CDCl_3$) 1.27 (t, $J=7.3$ Hz, 3H), 2.47 (s, 3H), 2.65 (t, $J=7.3$ Hz, 2H), 3.04 (t, $J=7.3$ Hz, 2H), 3.30 (s, 4H), 4.16 (q, $J=7.3$ Hz, 2H); ν_{max}(KBr)/cm^{-1} 2969 and 2921 (CH_2), 1731 (C=O), 1417 (C=C), 1183 and 1022 (C−O), 773 (C−S−C).

4,5-Ethylenedithio-4′-carbamoylmethylthio-5′-methylthiotetrathiafulvalene 1. In a 50 ml round-bottomed, short-necked flask fitted with a dropping funnel, **4** (781 mg, 1.65 mmol) and 2-bromoacetamide (1.13 g, 8.25 mmol) were dissolved in 50 ml of methanol–dichloromethane (9:1), the flask being cooled with an ice bath. To this solution was added dropwise sodium methoxide (357 mg, 6.60 mmol) in 5 ml of methanol with stirring under nitrogen. The resulting red solution was stirred for 12 h at room temperature. The mixture was filtered off with suction and the residue was dissolved in chloroform to remove sodium bromide. The orange solution was washed with 50 ml of saturated aqueous $NaHCO_3$ and 50 ml of water twice. The mixture was dried over anhydrous $MgSO_4$ and filtered, and then the solvent was evaporated. The crude product was recrystallized from chloroform to give **1** as orange needles (673 mg, 1.57 mmol, 98%); mp 139 °C; δ_H($CDCl_3$) 2.48 (s, 3H), 3.31 (s, 4H), 3.50 (s, 2H), 6.85 (s, 2H); ν_{max}(KBr)/cm^{-1} 3426, 3285, 3257 and 3184 (NH_2), 2976 and 2921 (CH_2), 1664 (C=O), 1601 (NH_2), 1483 (C=C, center), 1407 (C=C, peripheral), 1370 (C−N), 774 (C−S−C), 587 (N−C=O) (Calc. for $C_{11}H_{11}ONS_8$: C, 30.75; H, 2.58; N, 3.26; S, 59.69. Found C, 30.57; H, 2.57; N, 3.49; S, 60.00%).

General procedure for preparing iodine-doped samples of AMET

Doping of the crystals of AMET with iodine was carried out using the following procedure. The crystals of AMET were ground in a mortar with a pestle of agate. Then, the obtained crystallites were added to carbon tetrachloride containing a given amount of iodine and the suspension was stirred for 2 h at room temperature. The purple color of the suspension faded completely, indicating that the dissolved iodine had been homogeneously absorbed by the crystallites of AMET. The color of the crystallites of AMET changed from orange to black upon iodine doping. Doping of iodine into crystals of BEDT-TTF also carried out according to the same procedure. The doping ratio was evaluated *via* the increased weight of the doped sample.

X-Ray crystallographic analysis

A single crystal of AMET was mounted on a Rigaku AFC-5 four-circle diffractometer using graphite mono-chromatized Mo-Kα radiation ($\lambda = 0.7107$Å). The crystal system is orthorhombic, space group $Pca2_1$ (#29), and the cell constants refined with 20 reflections ($4 < 2\theta < 25^\circ$) are $a = 15.193(2)$, $b = 4.7566(8)$, $c = 23.472(3)$ Å, $V = 1696.2(4)$ Å^3. Intensity data were measured at ambient temperature; ω scan ($4 < 2\theta \leqslant 45^\circ$) and ω–2θ scan ($45 < 2\theta < 55^\circ$), scan speed 4 degrees min^{-1}, $0 < h < 19$, $0 < k < 30$, $0 < l < 6$. Three standard reflections (8 0 0, 0 14 0 and 0 4 2) were measured for every 100 reflections, with no significant variations throughout the data collection; among 2417 reflections measured ($4 < 2\theta < 55^\circ$), 2312 were unique ($R_{int} = 0.010$).

The structure was solved by direct methods using SIR92[11] and expanded using Fourier techniques.[12] The non-hydrogen atoms were refined anisotropically. The hydrogen atom coordinates were refined, their isotropic B values being fixed. The refinement of the structure was performed by a full-matrix least-squares method based on 1607 observed reflections [$I > 3.00\sigma(I)$]. Final refinement with anisotropic thermal factors for all atoms; 223 parameters, $R = 0.032$ and $R_w = 0.032$; $w = 1/\sigma^2(F_o)$; $S = 0.03$, max. (shift/e.s.d) = 0.09, max. and min. heights in final difference Fourier map 0.27, -0.25 e Å^{-3}. The atomic scattering factors used throughout the analysis were obtained from International Tables for X-ray Crystallography (1974). All calculations were performed using the teXsan crystallographic software package from the Molecular Structure Corporation.

Full crystallographic details, excluding structure factors, have been deposited at the Cambridge Crystallographic Data Centre (CCDC). See Information for Authors, *J. Mater. Chem.*, 1998, Issue 1. Any request to the CCDC for this material should quote the full literature citation and the reference number 1145/100.

Measurements of electric conductivity

Electric conductivities were measured by a four or two probe method. Gold wires (25 μm ϕ) were attached to the sample with gold paste. The sample was fixed in the chamber of a homemade cryostat and cooled slowly. The temperature was measured using a (0.03atom% Fe)-gold-Chromel thermocouple. The activation energies of the semiconducting samples were estimated by the slope of the straight line, obtained *via* a semilogarithmic plot of the conductivity *vs.* temperature. The pressure dependence of the conductivity of iodine-doped samples of AMET was measured by pressing a pellet of crystallites of AMET using a Be–Cu cell: DEMNUM S-20 (Daikin Industries Co, Ltd.) was used as a pressure transmitting medium.

Results and Discussion

Preparation of AMET

The preparative route to AMET **1** is shown in Scheme 1. The key reaction is the hetero-coupling between ethylenedithio ketone **2** and unsymmetrically substituted ketone **3** carrying an ethoxycarbonylethylthio group. After the coupling, the protecting group is efficiently removed by sodium methoxide *via* a retro-Michael addition mechanism (Scheme 2). The ethoxycarbonylethyl group is, therefore, considered to be an excellent protecting group for a thiolate in the coupling procedure.[13] The thiolate is reacted with 2-bromoacetamide to afford carbamoylmethylthio-substituted TTF derivative **1**. The yield of each step is reasonably high, and the total yield starting from $[Zn(dmit)_2]\cdot(Et_4N)_2$ **8** is 4–7%. Single crystals of neutral AMET were obtained by slow evaporation of a chloroform solution.

The donating ability of AMET was estimated *via* redox potentials determined by cyclic voltammetry. Two oxidation waves were measured: $E^{1/2}_{ox1} = 0.51$ V (reversible) and $E^{1/2}_{ox2} = 0.84$ V (irreversible). These values were practically the same as those of BEDT-TTF [$E^{1/2}_{ox1} = 0.51$ V (reversible) and $E^{1/2}_{ox2} = 0.85$ V (irreversible)]. This result suggests that introduction of a carbamoylmethyl group does not affect the donating ability of BEDT-TTF.

Crystal structure of AMET

The crystal structure of AMET is shown in Fig. 2. The long molecular axes of the AMET molecules are aligned in parallel along the *a* axis, being inclined by *ca.* 40°, and they are flipped alternately along the *c* axis. The conformation (τ_1, τ_2, τ_3, see

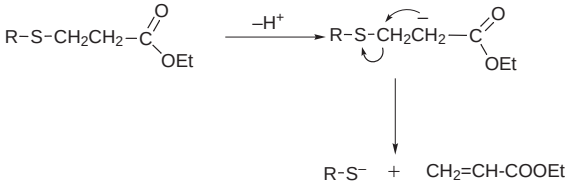

Scheme 2 Generation of a thiolate anion *via* retro-Michael addition

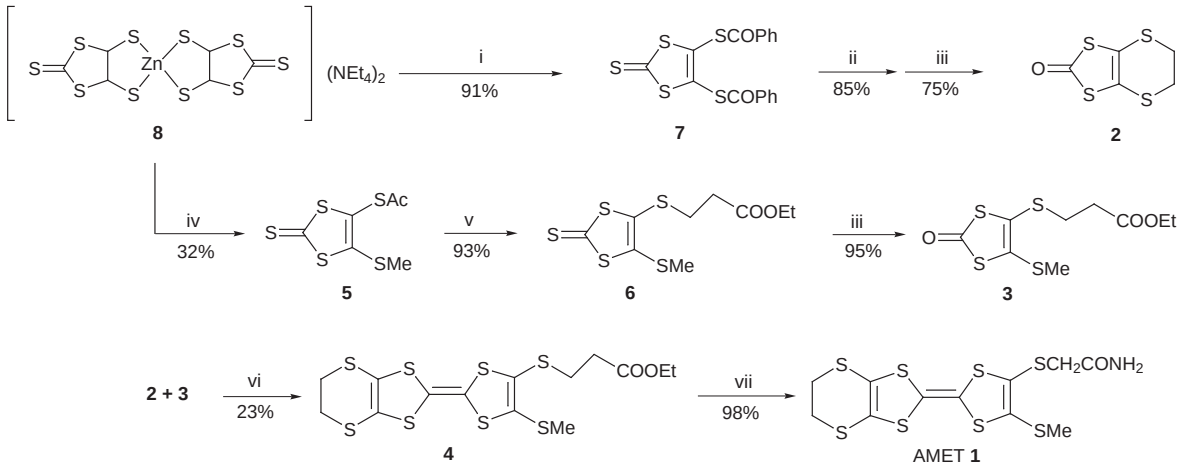

Scheme 1 *Reagents and conditions*: i, BzCl, acetone, room temp., 3 h; ii, NaOMe, MeOH, 0 °C, 1 h, then $BrCH_2CH_2Br$, MeOH, room temp., 12 h; iii, $Hg(OAc)_2$, $CHCl_3$, room temp., 3 h; iv, AcCl, acetone, −5 °C, 2 h, then MeI, acetone, room temp., 1 h; v, NaOMe, MeOH, 0 °C, 1 h, then $BrCH_2CH_2COOEt$, MeOH, room temp, 8 h; vi, $P(OEt)_3$, 110 °C, 3 h; vii, NaOMe, MeOH, 0 °C, 1 h, then $BrCH_2CONH_2$, MeOH, room temp., 4 h

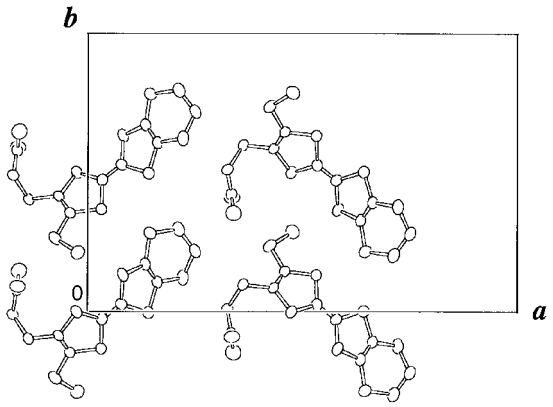

Fig. 2 Crystal structure of AMET viewed along the *b* axis

Fig. 3) of the carbamoylmethyl group of AMET is (−sc)-(+sc)-(+sc). The donor moiety has a concave shape, and the dihedral angles between the tetrathioethylene moieties of the central part and of the two edge parts are 22.3 and 13.1°, respectively (Fig. 3). No disorder was observed at the ethylenedithio group.

The carbamoylmethyl group forms a one-dimensional hydrogen-bonded chain along the *b* axis (Fig. 4). The hydrogen bond distance of N—H···O is 2.80 Å; this value is approximately an average distance for hydrogen bonds of amide groups.[14] As a result of these hydrogen bonds, the AMET moieties form columnar stacks along the *b* axis. The shortest S···S contact in this column is 3.76 Å. The distance is fairly

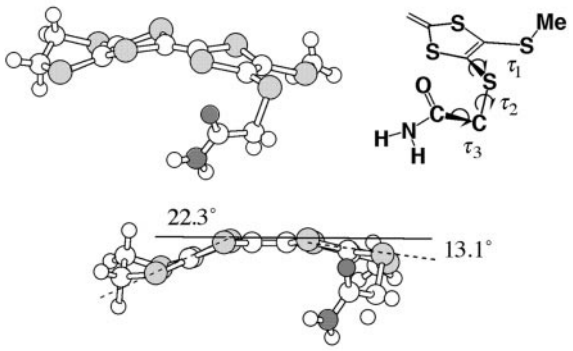

Fig. 3 Conformation of the carbamoylmethyl group of AMET

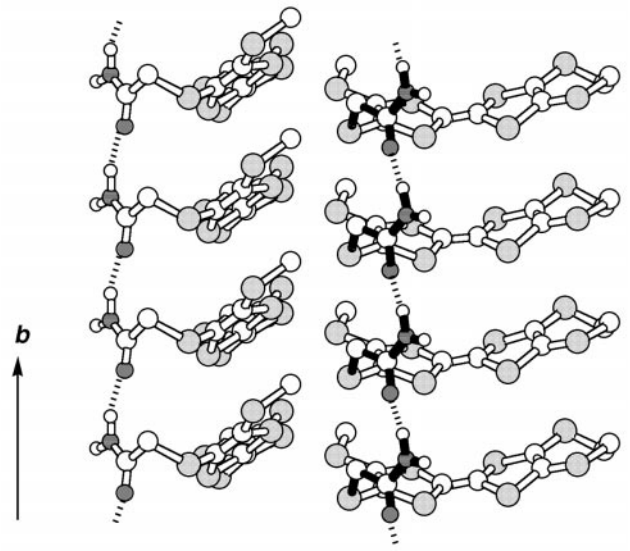

Fig. 4 Hydrogen-bonding scheme of AMET. The N—H···O distance is 2.80 Å

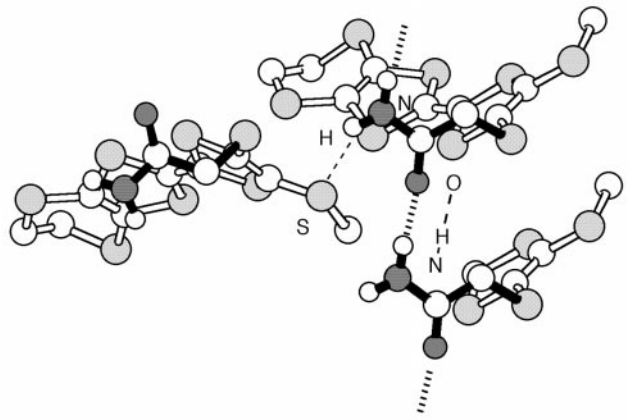

Fig. 5 The N—H···O hydrogen bond (2.80 Å; dotted line) and N—H···S intermolecular interaction (3.52 Å; broken line) of AMET

short in spite of the electronic repulsion between the π-electrons of the donor moieties. This structure is in sharp contrast to the herringbone structure of a neutral crystal of BEDT-TTF molecules.[3]

Primary amides, in general, form a double hydrogen-bonded chain utilizing the two hydrogen atoms of the amide group (Fig. 1).[5,6] In the case of the hydrogen-bonded crystal of AMET, however, only one of the hydrogen atoms of the amide group participates in a polymeric hydrogen bond. The other amide hydrogen is found in close proximity to the sulfur atom of a methylthio group belonging to an AMET molecule in an adjacent column. A weak N—H···S hydrogen bond is, thus, considered to be formed, with an N···S distance of 3.52 Å (Fig. 5). It should be noted that the hydrogen-bonded chain runs perpendicular to the stacking of the donors. Since the carbamoylmethyl group of AMET has conformational flexibility due to the methylene unit between the amide group and the donor moiety, the amide group can bend to give a (−sc)-(+sc)-(+sc) conformation.

Although the donor AMET moieties are stacked in parallel, the conductivity of the neutral crystal is not appreciably high, especially compared with the neutral crystal of tetrakis(decylthio)-TTF.[15] In the case of tetrakis(decylthio)-TTF, a one-dimensional stack of TTF moieties is achieved due to the dispersion force of the alkyl groups. This effect is called a 'fastener effect' in order to stress the importance of the dispersion force of the long alkyl chains. The S···S distance within a column of tetrakis(decylthio)-TTF molecules can be as short as 3.5 Å, and an exceptionally low resistivity (2.7×10^5 Ω cm) was recorded for a crystal of the neutral donor. Compared with tetrakis(decylthio)-TTF, the resistivity of neutral AMET is much higher (*ca.* 10^8 Ω cm). This may be explained by the slightly longer S···S contacts in neutral AMET and the inclined stacking of donor moieties.

Pressure dependence of IR spectra of undoped and iodine-doped AMET

In order to obtain information on the hydrogen-bonding pattern of the carbamoylmethyl group of AMET, especially under an external pressure, IR spectra of KBr pellets of neutral and iodine-doped AMET were recorded. The stretching modes of the amide group, ν_{NH} and $\nu_{C=O}$ (Amide I), and the deformation mode, δ_{N-C-O}, were chosen as key bands for this purpose.

The four N—H stretching bands, presumably resulting from site-splitting, were observed at 3426, 3285, 3257 and 3184 cm^{-1} (Fig. 6). Based on the assignments of acetamide,[16] the absorptions at 1664 and 587 cm^{-1} were assigned to the $\nu_{C=O}$ stretching (Amide I) and the N—C=O deformation (δ_{N-C-O}), respectively.

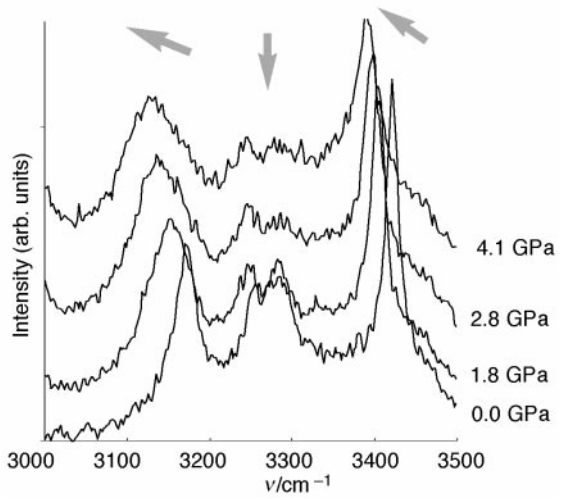

Fig. 6 Pressure dependence of IR spectrum of neutral AMET (ν_{NH} region)

When an external pressure was applied to the neutral sample, ν_{NH} at 3426 and 3184 cm^{-1} showed small shifts to lower wavenumber, Δk, of 37 and 58 cm^{-1}, respectively, at 4.1 GPa (Fig. 6), whereas the peaks at 3258 and 3257 cm^{-1} were relatively unaffected. On the other hand, $\nu_{C=O}$ at 1664 cm^{-1} showed a shift to higher wavenumber of 5 cm^{-1}. The δ_{N-C-O} at 578 cm^{-1} was also shifted to higher wavenumber by 60 cm^{-1}.

These results suggest that the N···O hydrogen bond distance becomes shorter when an external pressure was applied, and that the N—H hydrogen is shifted towards the oxygen atom, resulting in weakening of the N—H band. On the other hand, the δ_{N-C-O} (in plane) deformation peak showed a shift to higher wavenumber. This is because the force constant of the bending mode of the N—C=O group becomes larger due to the shorter hydrogen bond. Nakamoto *et al.* proposed a relation between a shift to lower wavenumber of the ν_{NH} stretching ($\Delta k/cm^{-1}$) and a shortening of the hydrogen-bonded distance (Δd/Å), $\Delta d = 7.7 \times 10^{-4} \times \Delta k$.[17] According to the above equation, the shrinkage in the N—H···O distance of AMET is estimated to be 0.04 Å at 4.1 GPa.

The pressure dependence of ν_{NH} and δ_{N-C-O} was also examined for the 5% iodine-doped sample. The ν_{NH} and δ_{N-C-O} absorptions showed shifts of -24 and $+66$ cm^{-1} respectively under 4.0 GPa. The shifts in ν_{NH} and δ_{N-C-O} are found to exhibit the same tendencies as those of the neutral sample. This result strongly suggests that the hydrogen-bonded scheme is not perturbed significantly, at least up to a doping ratio of 5%. For doping ratios higher than 45% a new absorption peak, assigned to $\nu_{C=O}$ of a more weakly hydrogen-bonded amide group, appeared at 1685 cm^{-1}. This may be explained by the partial disruption of the uniform polymeric hydrogen-bonded chain due to heavy doping. In other words, the hydrogen bonded chain supports the columnar stacking of donors as long as the doping ratio does not exceed *ca.* 45%.

It is well-documented that, in the IR spectrum of crystalline *N*-methylacetamide, the intensity of the small peak near amide II (1525 cm^{-1}) increases pronouncedly at lower temperatures.[18] This side-band peak is possibly assigned to the resonance line between the amide II and the lattice phonons, the intensity of which is enhanced due to the polaron along the hydrogen-bonded chain, although the origin of the side-band peak is still disputed. In crystals of AMET, such coupling has not been detected so far. If a coupling between polaronic migration and the transportational phenomena is observed, a new physical property might be explored, leading to a novel functionality characteristic of the hydrogen-bonded conductive materials.

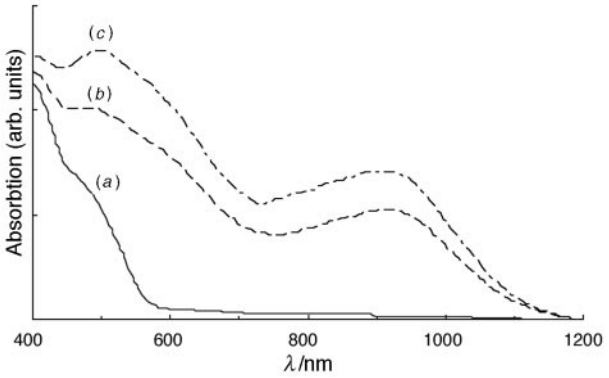

Fig. 7 UV–VIS spectra of AMET and iodine-doped samples; (*a*) neutral sample, (*b*) 12% I_2-doped sample, (*c*) 32% I_2-doped sample

UV–VIS spectra of undoped and iodine-doped AMET

The UV–VIS spectra of iodine-doped AMET were recorded in order to examine the electronic structure of the doped sample (Fig. 7). While the spectrum of neutral AMET showed absorption maxima at 400 and 490 nm, a broad absorption band at 930 nm was observed for the doped samples. This characteristic broad band can be assigned to the charge transfer band.

Besides the CT band, two absorption bands at 285 and 380 nm were recognized. The former band may be assigned to the absorption of I^- and the latter to I_3^-, respectively, judging from reference spectra for these species.[19] Thus, the doped iodine is converted to the counter ions I^- and I_3^-, which are considered to be in equilibrium with each other.

Effect of doping on the conductivities of neutral AMET and BEDT-TTF

The conductivities of pellets of neutral and iodine-doped AMET were measured as a function of the doping ratio (mol%). Although the conductivity of neutral AMET is as low as $\sigma_{rt} = ca.\ 10^{-8}$ S cm^{-1}, it is enhanced remarkably as the doping ratio increases. The conductivity of the 5% doped sample is 2×10^{-4} S cm^{-1}, 10^4 times larger than that of neutral AMET. The maximum value of the conductivity (1.2×10^{-1} S cm^{-1}) was obtained at a doping ratio of 45% (Fig. 8).

Although the maximum value of the conductivity of iodine-doped BEDT-TTF ($\sigma_{rt} = 4 \times 10^{-3}$ S cm^{-1}) is also obtained at a doping ratio of 45%, the value is 10^2 times smaller than the maximum value for iodine-doped AMET.

Some poly(vinyl-TTF) polymers have been synthesised in order to obtain conducting polymers carrying donor units.[20] Although these polymers were oxidized with bromine or TCNQ, the doped polymers exhibited poor conductivities ($\sigma_{rt} < 10^{-8}$ S cm^{-1}). The failure to obtain high conducting polymers may be ascribed to the difficulty of maintaining a face-to-face stack of donors along the backbone of the polymer. On the other hand, the donor units of AMET are arranged in a face-to-face stack along the hydrogen-bonded chain formed by the amide units, and the stacking structure is reasonably unperturbed by doping or the application of high pressures, as judged from the IR spectra of the doped samples.

Pressure dependence of the conductivities of iodine-doped AMET

The conductivities of 5 and 37% iodine-doped AMET samples under atmospheric pressure showed semiconducting behavior in the temperature range of 300–150 K. The activation energies of the 5 and 37% doped samples under atmospheric pressure were evaluated to be $E_a = 0.2$ and 0.09 eV, respectively.

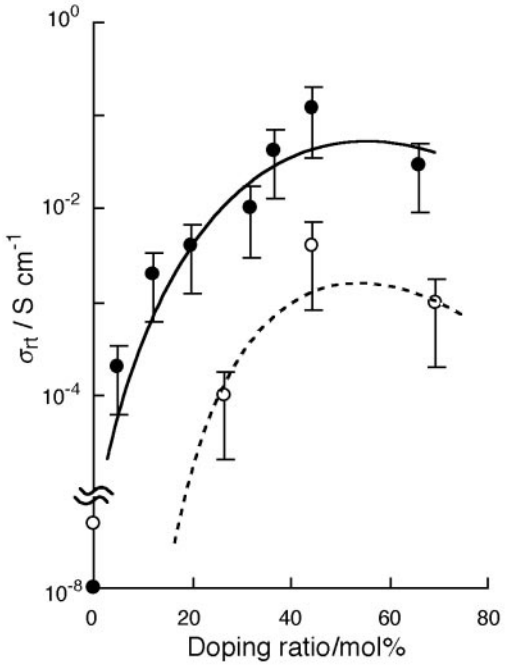

Fig. 8 Conductivity of the iodine-doped sample of (●) AMET and (○) BEDT-TTF

In the case of the 5% doped sample, the external pressure dependence of the conductivity was almost linear, and the conductivity under 1.0 GPa was about 3.5 times larger than that under atmospheric pressure (Fig. 9) on the left scale). However, the increase in conductivity of the 37% doped sample reached saturation at around 0.3 GPa (Fig. 9, on the right scale). The external pressure dependence of the activation energy of the iodine-doped sample was also examined (Fig. 10). The activation energy of the 5% doped sample decreased to $E_a = 0.1$ eV under 0.7 GPa, showing a minimum value at this pressure. On the other hand, the activation energy of the 37% doped sample was relatively unaffected by the application of external pressure.

The increase of the conductivity of iodine-doped AMET may be mainly rationalized by a decrease in the inter-donor distance within the stack, coupled with the shortening of the hydrogen bond distance of the amide groups. The degree of increase of the σ_{rt} value is of about the same order as those of the TTF–TCNQ, $(BEDT\text{-}TTF)_2Cu(NCS)_2$ and $(TMTSF)_2PF_6$

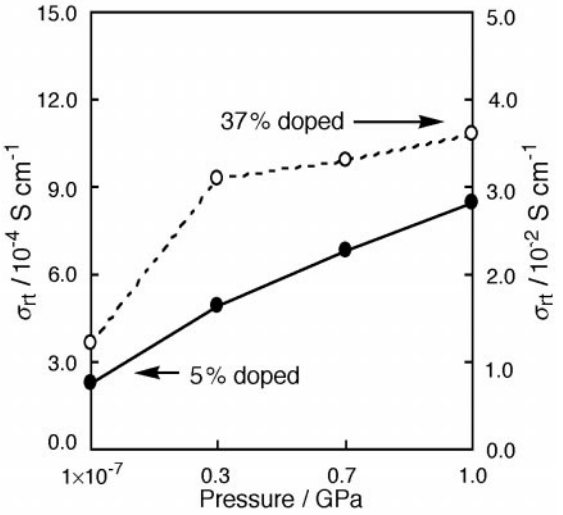

Fig. 9 External pressure dependence of conductivity of the (●) 5 and (○) 37% iodine-doped sample of AMET

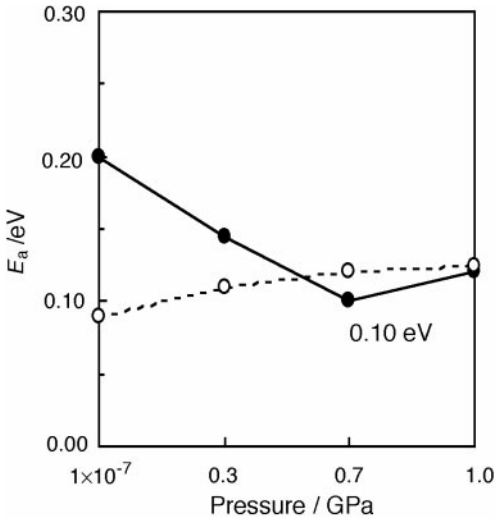

Fig. 10 External pressure dependence of activation energy of the (●) 5 and (○) 37% iodine-doped sample of AMET

salts.[21] Since the conductivity was measured using pellets, the possibility of a change in the contact resistance between crystallites cannot be ruled out.

Conclusion

According to the IR spectroscopic analysis of the hydrogen bond formed by the carbamoylmethyl group of AMET, this group appears to be effective in maintaining the hydrogen-bonded chain even in the doped sample under high pressure. Furthermore, the hydrogen bond distance is sensitive to the applied pressure. Such an effect may be derived from the polymeric hydrogen bond network, which is formed parallel to the π-stacking of the donor moieties.

It is to be stressed that the donor stacking is realized by simply introducing a carbamoylmethyl group into the donor moiety. This hydrogen-bonded molecular assembly composed of AMET is, therefore, appropriate for manifesting pressure-sensitive conducting properties under hole-doped conditions.

This work was partly supported by CREST of JST. The authors are indebted to Professor Tokura of the University of Tokyo, JRCAT, and Professor Moritomo of Nagoya University for the measurement of the IR spectra of AMET under high pressures. The authors also thank Dr Matsushita, Tokyo Metropolitan University, for discussions concerning the preparation of AMET.

References

1 For a review see: J. R. Fredericks and A. D. Hamilton, in *Comprehensive Supramolecular Chemistry*, ed, J. L. Atwood, J. E. D. Davies, D. D. MacNicol and F. Vögtle, Pergamon, Oxford, 1996, vol. 9, pp. 565–594.
2 M. Jørgensen, K. Bechgaard, T. Bjørnholm, P. Sommer-Larsen, L. G. Hansen and K. Schaumburg, *J. Org. Chem.*, 1994, **59**, 5877.
3 H. Kobayashi, A. Kobayashi, Y. Sasaki, G. Saito and H. Inokuchi, *Bull. Chem. Soc. Jpn.*, 1986, **59**, 301.
4 Y. Deng, A. J. Illies, M. A. James, M. L. McKee and M. Peschke, *J. Am. Chem. Soc.*, 1995, **117**, 420.
5 L. Leiaerowitz and A. T. Hagler, *Proc. R. Soc. Lond.*, 1983, **A388**, 133; C. C. F. Blake and R. W. H. Small, *Acta Crystallogr.*, 1972, **B28**, 2201; Q. Gao, G. A. Jeffrey, J. R. Ruble and R. K. McMullan, *Acta Crystallogr.*, 1991, **B47**, 742.
6 W. C. Hamilton, *Acta Crystallogr.*, 1965, **18**, 866; W. A. Denne and W. H. Small, *Acta Crystallogr.*, 1971, **B27**, 1094.
7 P. Blanchard, K. Boubekeur, M. Sallé, G. Duguay, M. Jubault, A. Gorgues, J. D. Martin, E. Canadell, P. Auban-Senzier, D. Jérome and P. Batail, *Adv. Mater.*, 1992, **4**, 579; A. S. Batsanov, M. R. Bryce, G. Cooke, A. S. Dhindsa, J. N. Heaton,

J. A. K. Howard, A. J. Moore and M. C. Petty, *Chem. Mater*., 1994, **6**, 1419; For a review see: M. R. Bryce, *J. Mater. Chem*., 1995, **5**, 1481.
8 G. Steimecke, R. Kirmse and E. Hoyer, *Z. Chem*., 1975, **15**, 28.
9 G. Steimecke, H-J. Sieler, R. Kirmse and E. Hoyer, *Phosphorus Sulfur*, 1979, **7**, 49.
10 A. Izuoka, R. Kumai and T. Sugawara, *Chem. Lett*., 1992, 285.
11 A. Altomare, M. C. Burla, M. Camalli, M. Cascarano, C. Giacovazzo, A. Guagliadi and G. Polidori, *J. Appl. Crystallogr*., 1994, **27**, 435.
12 *The DIRDIF-94 program system*, P. T. Beurskens, G. Admirraal, G. Beurskens, W. P. Bosman, R. de Gelder, R. Israel and J. M. M. Smits, in *Technical Report of the Crystallography Laboratory*, 1994, University of Nijmegen, The Netherlands.
13 G. Ono, M. M. Matsushita, A. Izuoka and T. Sugawara, *63rd National Meeting of the Chemical Society of Japan*, Abstracts, 1993, p. 147; Other protecting groups of a thiolate anion, see: N. Svenstrup, K. M. Rasmussen, T. K. Hansen and J. Becher, *Synthesis*, 1994, 809; J. Lau, O. Simonsoen and J. Becher, *Synthesis*, 1995, 521.
14 *The Hydrogen Bond*, ed. G. C. Pimentel and A. L. McClellan, W. H. Freeman and co., San Francisco, 1960, pp. 285–290; G. A. Jeffrey and W. Saenger, *Hydrogen bonding in biological structures*, Springer-Verlag, 1994, New York.
15 H. Inokuchi, G. Saito, P. Wu, K. Seki, T. B. Tang, T. Mori, K. Imaeda, K. Enoki, Y. Higuchi, K. Inaka and N. Yasuoka, *Chem. Lett*., 1986, 1263; N. Ueno, H. Kurosu, K. Seki, G. Saito, K. Sugita and H. Inokuchi, *Mol. Cryst. Liq. Cryst*., 1992, **218**, 171.
16 I. Suzuki, *Bull. Chem. Soc. Jpn*., 1962, **35**, 1279; T. Uno, K. Machida and Y. Saito, *Bull. Chem. Soc. Jpn*., 1969, **42**, 897.
17 K. Nakamoto, M. Margoshes and R. E. Rundle, *J. Am. Chem. Soc*., 1955, **77**, 6480.
18 G. Araki, K. Suzuki, H. Nakayama and K. Ishii, *Phys. Rev. B*, 1991, **43**, 12 662.
19 A. D. Awtrey and R. E. Connick, *J. Am. Chem. Soc*., 1951, **73**, 1842.
20 D. C. Green and R. W. Allen, *J. Chem. Soc*., *Chem. Commun*., 1978, 832; M. L. Kaplan, R. C. Haddon, F. Wudl and E. D. Feit, *J. Org. Chem*., 1978, **43**, 4642; C. U. Pittman Jr., M. Ueda and Y. F. Liang, *J. Org. Chem*., 1979, **44**, 3639.
21 A. Andrieux, H. J. Schulz, D. Jérome and K. Bechgaard, *J. Phys. Lett*., 1979, **40**, L-385; T. Takahashi, T. Ohyama, T. Harada, K. Kanoda, K. Murata and G. Saito, in *The Physics and Chemistry of Organic Superconductors*, ed. G. Saito and S. Kagoshima, Springer-Verlag, Berlin, 1990, pp. 107–110; P. Day, in *The Physics and Chemistry of Organic Superconductors*, ed. G. Saito and S. Kagoshima, Springer-Verlag, Berlin, 1990, pp. 8–14.

Paper 8/00509E; *Received* 19*th January* 1998